

Showcasing research from Professor Rai-Shung Liu's laboratory, Department of Chemistry, National Tsing Hua University, Hsinchu, Taiwan, ROC

Synthesis of two nitrogen-containing polyaromatic compounds through gold catalysis/DBU-promoted cyclizations

This work reports an efficient synthesis of novel benzo[7,8]indolizino[2,3,4,5-*ija*]quinazoline derivatives between 2-(2-ethynyl)acetonitriles and anthranils. The synthetic approach involves the initial formation of 7-formylindole intermediates that can be implemented by DBU to activate a novel indole-nitrile-aldehyde cyclization.

As featured in:



See Rai-Shung Liu *et al.*, *Chem. Commun.*, 2024, **60**, 4294.


 Cite this: *Chem. Commun.*, 2024, 60, 4294

 Received 9th January 2024,
 Accepted 19th March 2024

DOI: 10.1039/d4cc00113c


rsc.li/chemcomm

This work reports an efficient synthesis of novel benzo[7,8]-indolizino[2,3,4,5-*ija*]quinazoline derivatives between 2-(2-ethynyl-aryl)acetonitriles **1 and anthranils **2**. The synthetic approach involves the initial formation of 7-formylindole intermediates that can be implemented by DBU to activate a novel indole–nitrile–aldehyde cyclization.**

Nitrogen-doped polyarenes have attracted immense interest owing to their significance as electronic and pharmaceutical materials.^{1,2} Nevertheless, synthetic procedures to access such heteroaromatic compounds are long and tedious.^{1,2} Reported examples are largely limited to those polyarenes containing only one nitrogen atom. There is considerable interest in synthesizing polyarenes containing two or more nitrogen atoms, but little success is achieved toward material application.³ Fig. 1 shows those polyarenes containing two nitrogen atoms, which have optoelectronic applications.⁴ New convenient syntheses of such N-doped polyarenes are highly desired to expand the present small scope.

Scheme 1 (eqn (1)) shows a recent example of synthesizing fused four-membered benzenes such as benzo[7,8]indolizino[2,3,4,5-*ija*]quinoline (**I**) containing one nitrogen atom that is embedded in an indole moiety.⁵ We are aware that the two-nitrogen-containing analogues C₁₃H₈N₂, such as species **IV–VII**, have not been reported in the literature (eqn (4)). Incorporation of one additional nitrogen in polyaromatic frameworks can alter the optoelectronic properties. The LUMO–HOMO energy levels will be significantly decreased if a pyridine ring replaces a benzene ring.⁴ Gold catalysis proves to be a powerful tool to access all-carbon fused benzene rings;⁶ however, their applications to the synthesis of nitrogen-containing fused benzenes are not well explored. Recently, Hashmi reported⁷ gold-catalyzed synthesis of new indole

Synthesis of two nitrogen-containing polyaromatic compounds through gold catalysis/DBU-promoted cyclizations†

 Vikas Ashokrao Sadaphal, Tien-Lin Wu  and Rai-Shung Liu *

derivatives such as 2-amino-7-formylindole products (**III**) from the reactions of alkynes with anthranils (eqn (2)). So far, this catalytic reaction has no imminent impact on materials and medicinal chemistry. This work reports the new development of this catalytic reaction to access two-nitrogen containing fused benzenes such as benzo[7,8]indolizino[2,3,4,5-*ija*]quinazoline (**4a**), which is unprecedented in the literature (eqn (3)). This reaction sequence comprises two separate steps involving the initial treatment of 2-(2-ethynylaryl)acetonitriles **1a** with anthranil **2a** with a suitable gold catalyst in hot DCE, followed by a novel DBU-promoted⁸ indole–nitrile–aldehyde cyclization; intermediate **3a** can be isolated and well characterized.

In material applications, 7-phenyl-7*H*-pyrido[3,2-*c*]carbazole (**VIII**)^{9a} has applications in OLED devices (Fig. 1). 4,7-Diphenyl-1,10-phenanthroline (BPhen, **IX**)⁴ is a commonly used electron transport material (ETM) with good hole-blocking ability. Tetraphenylbis(indolo[1,2-*a*])quinoline (TPBIQ, **X**)^{9b} has found application as an organic field transistor.

The reactions of 2-(2-ethynylaryl)acetonitriles **1a**¹⁰ (2.0 equiv.) with anthranil **2a** (1.0 equiv.) are optimized using various gold catalysts; the results are shown in Table 1. Alkyne substrate **1a** was used in an excessive amount because protracted heating in this catalysis will cause slow alkyne decomposition. The reaction using IPrAuCl (10 mol%)/AgNTf₂ (10 mol%) in hot DCE for a period of time (*t*₁ = 20 h) ensured a nearly complete reaction; subsequently, DBU (1.0 equiv.) was added to the same solution with continuing heating (80 °C, *t*₂ = 24 h). After workup, a new product **4a** was isolated in 56% yield (entry 1). Other gold catalysts, LAuCl/AgNTf₂ [L = PPh₃ and P(OPh)₃], gave the same product **4a** in 45 and 37% yields, respectively (entries 2 and 3). Next, we altered the silver

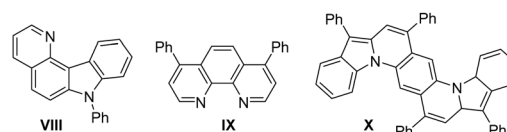
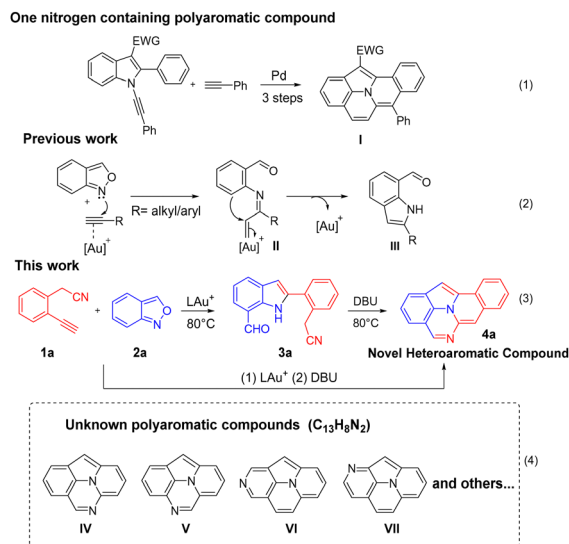


Fig. 1 N-heterocycles as electronic materials.

Department of Chemistry, National Tsing Hua University, Hsinchu, Taiwan, Republic of China. E-mail: rslu@mx.nthu.edu.tw

 † Electronic supplementary information (ESI) available. CCDC 2283773, 2283774, 2288008, 2290023, 2292226, 2301524, 2301525 and 2301731. For ESI and crystallographic data in CIF or other electronic format see DOI: <https://doi.org/10.1039/d4cc00113c>

Scheme 1 Target for N-doped polyaromatic compounds.

Table 1 Optimization of the reaction conditions

Entry	Catalyst	Solvent	Time		Yield ^b (%)	
			t_1/t_2 (h)	4a	2a	
1	IPrAuCl/AgNTf ₂	DCE	20/24	56	8	
2	PPh ₃ AuCl/AgNTf ₂	DCE	22/23	45	13	
3	(PhO) ₃ PAuCl/AgNTf ₂	DCE	23/21	37	16	
4	IPrAuCl/AgSbF ₆	DCE	20/23	50	9	
5	IPrAuCl/AgOTf	DCE	24/19	33	18	
6	IPrAuCl/NaBARF	DCE	23/21	41	11	
7 ^c	IPrAuCl/AgNTf ₂	DCE	19/26	69	—	
8 ^c	IPrAuCl/AgNTf ₂	Ph-CF ₃	24/21	38	16	
9 ^c	IPrAuCl/AgNTf ₂	Toluene	23/17	20	63	
10 ^c	IPrAuCl/AgNTf ₂	ACN	18/00	—	77	
11	IPrAuCl	DCE	24/00	—	71	
12	AuCl ₃	DCE	24/20	39	15	
13	AgNTf ₂	DCE	16/00	—	83	

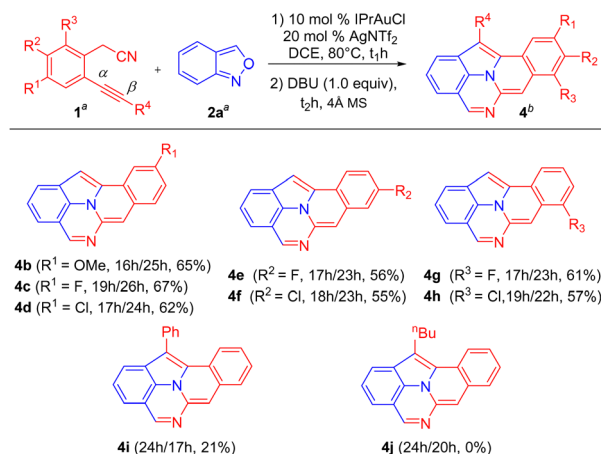
^a Reaction conditions: **1a** (1.6 mmol), **2a** (0.8 mmol), gold catalyst (10 mol%), DBU (1.0 equiv.) in solvent (3.0 mL) under a N₂ atmosphere. ^b Product yields are obtained after purification from a silica column. ^c Additional 10 mol% AgNTf₂. DCE = 1,2 dichloroethane. ACN = acetonitrile.

salts for IPrAuCl (AgX, X = SbF₆ and OTf), further affording **4a** in 50 and 33% yields, respectively (entries 4 and 5). Furthermore, silver-free IPrAuCl/NaBARF (BARF = B[3, 5-(CF₃)₂C₆H₃]₄) was prepared, to yield our target **4a** in 41% yield (entry 6). Notably, adding AgNTf₂ (10 mol%) to this IPrAuCl/AgNTf₂ (10 mol%) system increased the yield of **4a** to 69% (entry 7). With this new IPrAuCl/AgNTf₂ composition, the yields of compounds **4a** in different solvents were as follows (entries 8–10): CF₃C₆H₅ (38%), toluene (20%), and acetonitrile (0%). IPrAuCl without silver salts

was inactive under the same reaction conditions (entry 11). AuCl₃ was also less efficient, giving **4a** in 39% yield (entry 12). AgNTf₂ alone was catalytically inactive as well (entry 13). The molecular structure of compound **4a** was characterized by X-ray diffraction;¹¹ its ORTEP image is shown in Table 1. Our reaction sequence involves readily available reagents **1a** and **2a**, whereas the method in eqn (1) employs highly functionalized indoles as the starting reagent.

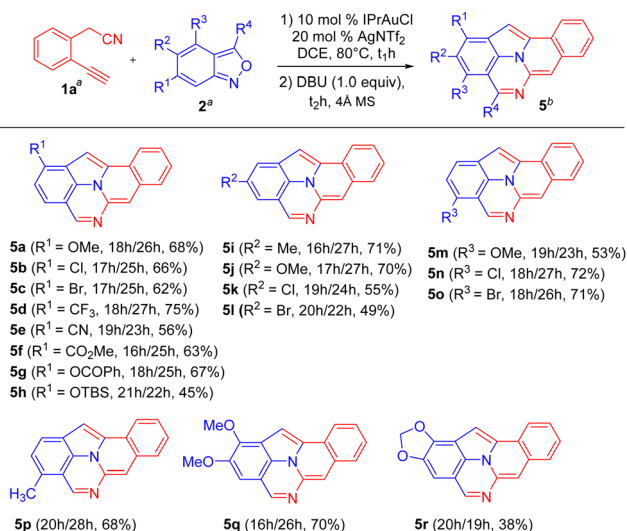
The generality of this new catalysis is assessed using various 2-(2-ethynyl)acetonitriles **1** and anthranil **2a**; the results are summarized in Scheme 2. The operation used IPrAuCl/AgNTf₂ in 10 mol% and 20 mol%, respectively, in the first step, and DBU (1.0 equiv.) in the second step. For substrates **1b–1d** bearing various 5-phenyl substituents ($R^1 = \text{OMe, F, and Cl}$), their standard operations yielded the desired products **4b–4d** in 62–67% yields. We prepared additional substrates **1e** and **1f** containing 4-phenyl substituents ($R^2 = \text{F and Cl}$), which delivered the desired products **4e** and **4f** in 56 and 55% yields, respectively. We also prepared substrates **1g** and **1h** bearing 3-phenyl substituents ($R^3 = \text{F and Cl}$), and the corresponding products **4g** and **4h** were obtained in 61 and 57% yields, respectively. Substrate **1i**, bearing a phenylethynyl group, afforded the desired product **4i**, albeit with only 21% yield. Another internal alkyne substrate, **1j** ($R^1 = n\text{-butyl}$), failed to form the C(2)-substituted 7-formylindole intermediate through the C(α)-addition. The low efficiency of internal alkyne substrates is due to a distinct C(β)-regioselectivity for the anthranil attack on gold- π -alkyne, whereas our target **4** is produced from the alkynyl C(α)-regioselectivity. This assessment is further manifested by our control experiments (*vide infra*, eqn (5)–(7)).

Scheme 3 provides the outcome of the reaction of standard alkyne substrate **1a** with various anthranils **2**. A wide range of anthranils **2b–2h** bearing various functional groups, including $R^1 = \text{OMe, Cl, Br, CF}_3, \text{CN, CO}_2\text{Me, OCOPh, and OTBS}$, could produce the desired products **5a–5h** in 45–75% yield; herein,



Scheme 2 Substrate scope for 2-(2-ethynyl)acetonitriles. ^a Reaction conditions: **1** (1.6 mmol), **2a** (0.8 mmol), IPrAuCl (10 mol%), AgNTf₂ (20 mol%), and DBU (1.0 equiv.) in solvent (3.0 mL) under a N₂ atmosphere. ^b Product yields are obtained after purification from a silica column.



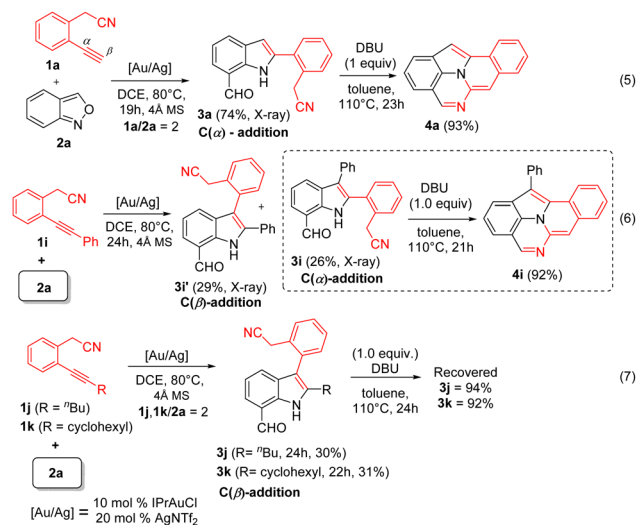


Scheme 3 Substrate scope with respect to the anthranils. ^a Reaction conditions: **1a** (1.6 mmol), **2** (0.8 mmol), IPrAuCl (10 mol%), AgNTf₂ (20 mol%), DBU (1.0 equiv.) in solvent (3.0 mL) under a N₂ atmosphere. ^b Product yields are obtained after purification from a silica column.

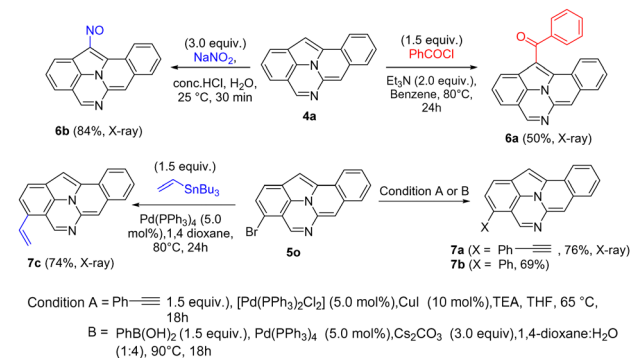
only product **5h** ($R^1 = \text{OTBS}$) was obtained in low yield (45%). For anthranils **2i–2l** containing $R^2 = \text{Me}$, OMe, Cl, and Br, their reactions gave the desired products **5i–5l** in 49–71% yields. Additional anthranils **2m–2o** bearing $R^3 = \text{OMe}$, Cl, and Br, delivered similar products **5m–5o** in 53–72% yields. For anthranil **2p** with $R^4 = \text{Me}$, the corresponding product **5p** was produced in 68% yield. For disubstituted anthranils **2q** and **2r**, bearing R^1 , $R^2 = \text{OMe}$ and OCH₂O, this gold catalysis afforded the desired products **5q** and **5r** in 70 and 38% yields, respectively. In Scheme 3, only a few products such as **5h**, **5l** and **5r** were produced in low yields (< 50%).

Control experiments were conducted to study the effect of alkyne substrates. The gold-catalyzed reaction between 2-cyanomethyl-1-ethynylbenzene **1a** (2.0 equiv.) and anthranil **2a** yielded C(2)-substituted 7-formylindole **3a** in 74% yield (Scheme 4, eqn (5)). The molecular structure of compound **3a** was elucidated by X-ray diffraction.¹¹ A further treatment of this species with DBU (1.0 equiv.) in hot toluene yielded the desired product **4a** in 93% yield. For substrate **1i** bearing an internal alkyne, two regioisomeric 7-formylindoles **3i'** and **3i**, were obtained instead (eqn (6)). Their molecular structures were characterized by X-ray diffraction.¹¹ Only the C(α)-addition product such as C(2)-substituted 7-formylindole **3i** was active towards the DBU-promoted cyclization to yield our target **4i** in 92% yield. Finally, we prepared alkyl-substituted alkynes **1j** and **1k**, herein the C(β)-addition products, *i.e.*, C(3)-substituted 7-formylindole **3j** and **3k**, were obtained in low yields (eqn (7)). Importantly, these two species are chemically robust in the presence of DBU.

Scheme 5 depicts the chemical functionalization of compounds **4a** and **5o**. Treatment of species **4a** with PhCOCl (1.5 equiv.) yielded a new acylation product **6a** in 50% yield. Treatment of compound **4a** with HCl/NaNO₂, produced a nitrosyl-derived product **6b** in 84% yield. Bromo-containing



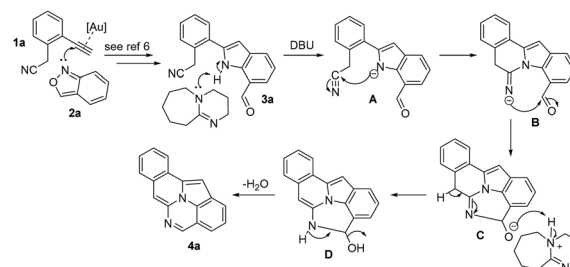
Scheme 4 Control experiments.



Scheme 5 Chemical functionalization.

species **5o** was active towards the Sonogashira reaction to yield the cross-coupling product **7a** in 76% yield. The Suzuki–Miyaura cross-coupling of compound **5o** with phenylboronic acid led to the formation of product **7b** in 69% yield. Furthermore, the Stille–Miyaura reaction on species **5o** with tributyl(vinyl)tin, delivered product **7c** in 74% yield. The molecular structures of **6a**, **6b**, **7a** and **7c** were elucidated using X-ray diffraction.¹¹

This gold catalysis and DBU-promoted cyclization involves an initial formation of 7-formylindole **3a** (Scheme 6); its formation mechanism follows an early proposal in Hashmi's



Scheme 6 A plausible reaction mechanism.



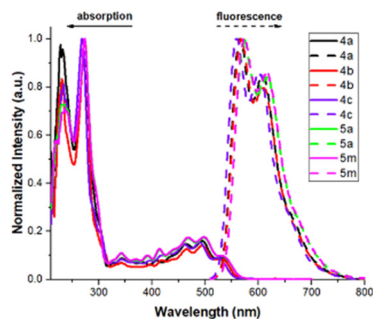


Fig. 2 Emission and absorption spectra.

work⁶ (see eqn (2)). The second step comprises an intramolecular reaction among indole, nitrile and aldehyde; such a three-component cyclization is unprecedented in the literature. We postulate an initial deprotonation of the indole N-H group of intermediate **3a** to form an amide anion **A** that attacks the nitrile group to generate an imino anion **B**; this step does not require a gold catalyst according to our control experiment in eqn (5). A final intramolecular cyclization is likely to occur between this imino anion **B** and the aldehyde to generate an oxy anion **C**, which upon protonation by the DBU/H⁺ complex will generate the last intermediate **D**. A final aromatization of this intermediate **D** delivers the observed product **4a**.

Photophysical properties of representatives **4a–4c**, **5a** and **5m** were measured to examine their potential material applications. Fig. 2 shows the electronic absorption and emission spectra, and Table S1 (see ESI[†]) shows their corresponding wavelengths, absorption efficiencies and Stokes shifts. All these compounds have very similar values despite various substituents (Cl, F and OMe) on three different benzene rings. One strong absorption band is observed at 268–274 nm, corresponding to π – π^* transition with large coefficients ($\log \epsilon = 4.47$ – 4.91). The emission spectra are centered at 565–572 nm in the yellow–orange region. Notably, the Stokes shifts are quite large up to 291 – 299 nm^{–1}, which reflects a fast relaxation process from the initial state to the emissive state.

In summary, we have developed new gold catalysis between 2-cyanomethyl-1-ethynylbenzene with anthranils to construct benzo[7,8]indolizino[2,3,4,5-*ij*a]quinazoline frameworks. In this reaction sequence, anthranils attack the gold- π -alkyne intermediate at the alkyne C(α)-regioselectivity forming 7-formylindole intermediates that can be isolated and characterized. Internal alkyne substrates are not efficient because the alkyne C(β)-regioselectivity occurs to yield 7-formylindole intermediates that are not active towards the DBU-activated cyclizations. The use of readily available substrates **1** and **2** to access

two-nitrogen containing fused benzenes highlights the significance of this work.

The authors thank the National Science and Technology Council (NSTC 112-2113-M-007-013), Taiwan, for supporting this work.

Conflicts of interest

There are no conflicts to declare.

Notes and references

- (a) G. Zeni and R. C. Larock, *Chem. Rev.*, 2006, **106**, 4644–4680; (b) L. Xiao, H. Lan and J. Kido, *Chem. Lett.*, 2007, **36**, 802; (c) U. H. F. Bunz, J. U. Engelhart, B. D. Lindner and M. Schaffroth, *Angew. Chem., Int. Ed.*, 2013, **52**, 3810–3821; (d) X. F. Wu, H. Neumann and M. Beller, *Chem. Rev.*, 2013, **113**(1), 1–35; (e) M. Stepien, E. Gonka, M. Zyla and N. Sprutta, *Chem. Rev.*, 2017, **117**, 3479–3716; (f) S. Hiroto, *Chem. – Asian J.*, 2019, **14**(15), 2514–2523; (g) Z. Zeng, H. Jin, K. Sekine, M. Rudolph, F. Rominger and A. S. K. Hashmi, *Angew. Chem., Int. Ed.*, 2018, **57**, 6935–6939; (h) Z. Zeng, H. Jin, M. Rudolph, F. Rominger and A. S. K. Hashmi, *Angew. Chem., Int. Ed.*, 2018, **57**, 16549–16553; (i) K. P. Kawahara, W. Matsuoka, H. Ito and K. Itami, *Angew. Chem., Int. Ed.*, 2020, **59**, 6383–6388; (j) A. Borisov, Y. K. Maurya, L. Moshniha, W.-S. Wong, M. Zyla-Karwowska and M. Stepien, *Chem. Rev.*, 2022, **122**, 565–788.
- (a) M. Ishikura, T. Abe, T. Choshi and S. Hibino, *Nat. Prod. Rep.*, 2013, **30**, 694; (b) L. W. Ye, X. Q. Zhu, R. L. Sahani, Y. Xu, P. C. Qian and R.-S. Liu, *Chem. Rev.*, 2021, **121**, 9039–9112; (c) Y. Li, J. Jin, W. Fan and D. Huang, *Org. Lett.*, 2023, **25**, 8284–8289; (d) S. Nam and I. Kim, *J. Org. Chem.*, 2023, **88**, 745–754.
- (a) M. Tasiar, M. Chotkowski and D. T. Gryko, *Org. Lett.*, 2015, **17**(24), 6106–6109; (b) B. Alcaide, P. Almendros, I. Fernandez, F. Herrera and A. Luna, *Chem. – Eur. J.*, 2018, **24**, 1448–1454; (c) J. Qiao, X. Jia, P. Li, X. Liu, J. Zhao, Y. Zhou, J. Wang, H. Liu and F. Zhao, *Adv. Synth. Catal.*, 2019, **361**, 1419–1440; (d) Y. Zhang, S. H. Pun and Q. Miao, *Chem. Rev.*, 2022, **122**, 14554–14593.
- D. Chen, S.-J. Su and Y. Cao, *J. Mater. Chem. C*, 2022, **10**, 9565.
- K. Alam, S. W. Hong, K. H. Oh and J. K. Park, *Angew. Chem., Int. Ed.*, 2017, **56**, 13387–13391.
- (a) C. F. Shu, C.-B. Chen, W.-X. Chen and L.-W. Ye, *Org. Lett.*, 2013, **15**, 5542–5545; (b) C. Zhang, K. Hong, C. Pei, S. Zhou, W. Hu, A. S. K. Hashmi and X. Xu, *Nat. Commun.*, 2021, **12**, 1182.
- H. Jin, L. Huang, J. Xie, M. Rudolph, F. Rominger and A. S. K. Hashmi, *Angew. Chem., Int. Ed.*, 2016, **55**, 794–797.
- (a) S. K. Guchhait, G. Priyadarshani and N. M. Gulghane, *RSC Adv.*, 2016, **6**, 56056; (b) R. R. Zalte, A. A. Festa, N. E. Golantsov, K. Subramani, V. B. Rybakov, A. V. Varlamov, R. Luque and L. G. Voskressensky, *Chem. Commun.*, 2020, **56**, 6527–6530.
- (a) C. J. Shin, D. M. Kang, M. S. Kang, N. H. Lee, H. G. Lee, H. K. Jung and M. Y. Chae, *PCT Int. Appl.*, WO 2013089424 A1 20130620, 2013; (b) L. Zhu, E.-G. Kim, Y. Yi, E. Ahmed, S. A. Jenekhe, V. Coropceanu and J.-L. Bredas, *J. Phys. Chem. C*, 2010, **114**, 20401.
- For gold-catalyzed reactions of alkyne substrate **1** with the pyridine-based oxide, see: S.-N. Karad and R.-S. Liu, *Angew. Chem., Int. Ed.*, 2014, **53**, 5444–5448.
- Compound **3a** (CCDC 2283774), **3i** (CCDC 2292226), **3i'** (CCDC 2290023), **4a** (CCDC 2283773), **6a** (CCDC 2288008), **6b** (2301731), **7a** (CCDC 2301524) and **7c** (CCDC 2301525) contain the supplementary crystallographic data for this paper[†].

